The International Journal of Advanced Manufacturing Technology (2025) 140:1945–1961
https://doi.org/10.1007/s00170-025-16244-w

ORIGINAL ARTICLE

Rheological parameter ranges for 3D printing sustainable mortars using a new low-cost rotational rheometer

Sara Alonso-Cañon[1] · Alejandro Alonso-Estébanez[1] · Adrian Isidro Yoris-Nobile[1] · Ana Brunčič[2] · Elena Blanco-Fernandez[1] · Laura Castanon-Jano[1]

Received: 20 January 2025 / Accepted: 31 July 2025 / Published online: 28 August 2025

Abstract
Concrete 3D printing in the field of construction is rapidly developing in recent years. Some key aspects of mortars used in 3D printing include good extrudability and sufficient load-bearing capacity to support their own weight during the printing process. Thus, the rheological properties of the fresh mortar should be determined since they have to be comprised between certain values to make mortars suitable for 3D printing. In this study, a low-cost rotational rheometer has been developed to obtain the rheological characteristics of different mortar mixtures apt for 3D printing. In order to validate it, numerical simulations have been undertaken, which have shown a good correlation between the experimental and analytical results. Furthermore, a comparison with another commercial rheometer has been conducted using a mortar without fibers and a common testing protocol, showing results with similar variability to other proficiency tests undertaken with cement pastes. In addition, the rheological behavior of various sustainable mixtures incorporating recycled materials and different types of fibers was studied. The article further examines how the types, lengths, and percentages of fibers influence rheological parameters, establishing ranges suitable for 3D printing.

Keywords Rheology · Fibers · 3D concrete printing · 3D mortar printing · Yield stress · Viscosity · Rheometer

1 Introduction

Additive manufacturing, more commonly known as 3D printing, has been in continuous advance and development since the 1980 s [1]. In the construction field, and in the particular case of concrete 3D printing, this technique began to be explored since the late 1990 s [2] especially when non-conventional shapes are required.

In the development of 3D printing in construction, fresh state properties of concrete play a crucial role, being more critical than in cast concrete. 3DCP (3D concrete printed) must have good flowability and workability, allowing the material to be pumped and extruded through the nozzle. Nevertheless, once the layers have been extruded, they must have sufficient self-supporting capacity to maintain their shape and support the weight of the layers that are subsequently deposited. Due to this, the rheological properties of fresh concrete are fundamental parameters that must be analyzed and controlled in order to predict whether a concrete mix is apt for 3D printing.

The rheological behavior of concrete in a fresh state is generally considered to conform to the Bingham model [3, 4] and is given by the following equation: $\tau = \tau_o + \eta\dot{\gamma}$. τ_o is the dynamic yield stress and η is commonly referred as plastic viscosity [5, 6]. These parameters are derived from a shear stress–strain rate descending fit line from a flow curve obtained with a rheometer. Dynamic yield stress and plastic

✉ Elena Blanco-Fernandez
elena.blanco@unican.es

Sara Alonso-Cañon
alonso1alonso@gmail.com

Alejandro Alonso-Estébanez
alejandroalonsoes@hotmail.com

Adrian Isidro Yoris-Nobile
adrianyoris84@gmail.com

Ana Brunčič
ana.bruncic@zag.si

Laura Castanon-Jano
laura.castanon@unican.es

[1] GITECO Research Group, Universidad de Cantabria, Av. de los Castros 44, 39005 Santander, Spain

[2] Slovenian National Building and Civil Engineering Institute (ZAG), Dimičeva Ulica 12, 1000 Ljubljana, Slovenia

viscosity will be referred to from now on as yield stress and viscosity, to simplify. Both parameters, yield stress and viscosity, are key to predict the suitability of mortars and concretes used for 3D printing. To calculate these parameters, different types of rotational rheometers have been developed in the 1990 s, such as ICAR[7], two-points [4, 8], BML [9] and BTRHEOM [10, 11], some of them having derived in commercial rheometers. All of them, in spite of having different shapes and geometries, are based on the same principle: to correlate torque and rotational speed (measured magnitudes from the equipment) with shear stress and shear strain rate by using either a standard viscous fluid or with analytical formulas. Several authors have undertaken tests with rotational rheometers that have allowed them to obtain values of both yield stress and viscosity for 3DCP. Jayathilakage et al. [12] made a comparison with different types of rheometers, verifying that torque rheometers provide correct values of rheological properties, although yield stress and viscosity were equipment dependent somehow.

Brower and Ferraris [13] is one of the oldest interlaboratory tests of rheometers carried out with different concretes, equipment, and test methods. Twelve different concrete formulations and five rheometers were used in the interlaboratory test campaign. Aggregate size ranged between 0 to 20 mm maximum depending on the formula and admixtures used in order to modify viscosity; however, no specific information about admixture brands was provided, so it is not possible to replicate. Besides, numerical simulations were not carried out either. Values of yield stress and viscosity were quite dispersed among rheometers. Haist et al. [14] developed a large interlaboratory study on rheological properties using different rotational rheometers that was carried out using a cement paste standard formulation containing Cem I 42.5 R and distilled water. The values of torque and speed for the different rheometer types and geometries were converted through analytical formulations into yield stress and viscosity assuming a Bingham model. Average values reported for this cement paste were 40.0 ± 11 Pa and 0.50 ± 0.12 Pa•s for the yield stress and viscosity, respectively. These results were not compared with numerical simulations, though. Also, in the majority of these studies, the authors used commercial rheometers, which are, generally speaking, quite costly.

In relation to numerical simulations that model rotational rheometers with mortars, there are very few experiences in the current state of the art that compare rheological parameters (yield stress and viscosity) obtained from a rheometer with those from numerical simulations assuming a Bingham model. Eslami et al. [15] compared the torque obtained from two types of rheometers (vane-in-cup and coaxial cylinders) versus the values obtained from CFD numerical simulations. The material used was not a mortar, but instead, two types of silicone oils, which were considered Newtonian fluids for both analytical models and simulations. Wallevik et al. [16] developed a new type of rotational rheometer that was a sort of hybrid of a vane and coaxial rheometer apt for concretes, with the purpose of avoiding aggregate segregation. Numerical simulations were performed in order to establish correlation graphs that could be used to calculate yield stress and viscosity by knowing H and G. These two parameters, H and G, were obtained from the line that depicts torque vs. rotational frequency of the rheometer, where H was the slope of the line and G the intersection with the ordinate axis. Using two types of concretes (aggregate maximum size 16 and 32 mm respectively) and a mortar (aggregate maximum size 8 mm), comparisons of the yield stress and viscosity of this rheometer with another axial rheometer were conducted, showing similar rheological results. Nevertheless, an analytical model was not applied to calculate the yield stress and viscosity of the rheometer test parameters (torque and speed) and, thus, to compare also with the numerical simulation. Overall, in the particular case of rotational 4-vane rheometers, there are no previous experiences that compare laboratory tests and simulations on 3D printing mortars.

In relation to 3D printing mortar formulations, despite the fact that there is a reasonably large amount of publications showing their mechanical performance and rheological parameters, there is still a lack of sufficient investigations concerning sustainable 3DCP [17]. In this sense, it is relevant to provide more experiences that enlarge the catalogue of sustainable 3DCP materials, including mechanical properties, rheological properties, cost, and environmental performance. In this sense, this work provides a set of formulations that uses both low-linker cement and geopolymer as binders, natural aggregate, but also construction and demolition waste (CDW) and even crushed shells as aggregates, analyzing their rheological parameters. Details on life cycle assessment (LCA), mechanical properties, and cost can be consulted in a previous work published by the authors [18].

The main contributions of this paper to the current state of the art are as follows: (i) the development of a low-cost, 4-blade rotational rheometer for mortar testing, which relies on analytical formulas validated through comparisons with numerical simulations and a commercial rheometer; and (ii) the analysis of how new sustainable 3D concrete printing (3DCP) formulations—based on either cement or geopolymer mortars, with or without fibers—affect yield stress and viscosity.

2 Materials and equipment

2.1 Mortars without fibers

In this project, 3D printable mortars of both cements and geopolymers were developed. For the elaboration of

these, two types of cements were used: Cem III/B 32.5 N-SR and Cem III/A 42.5 N. Fly ash was also used in both types of mixtures, being used as the main binder in the case of geopolymers and to give more continuity to the granulometric curve in the case of cements. The limestone aggregate was used in two fractions: [0–3] mm and [0–1] mm. In addition, in order to develop more sustainable dosages, partial substitutions of these aggregates were made with other recycled ones. The recycled aggregates used were the following: crushed seashells, car windshield breakage, and construction and demolition waste (CDW). As workability-modifying additives, the following were used: MasterSure950, a superplasticizer (SP); MasterRoc MS 685, a suspension of precipitated nanosilica (N.S.); and MasterRoc MS 610, a densified microsilica (M.S.). Finally, in the geopolymer mixtures, sodium hydroxide (NaOH) was used as an activator, with molar concentrations of 10 M and 14 M. The mixtures used are listed in Table 1.

2.2 Mortars with fibers

In dosage 1, which was used as reference, different types of fibers were incorporated to analyze how their incorporation affects the rheological behavior of the printable mixtures. The fibers that were tested were the following: aramid, carbon, cellulose, glass, zylon, and textile. These range from recycled fibers, such as textiles, to natural fibers, such as cellulose, to zylon fibers, which are the fibers with the highest elastic modulus in the market. The characteristics of the fibers can be found in Table 2. In order to carry out a broader analysis, apart from analyzing how the types of fibers affect, different ratios of fibers were also incorporated, and for some samples, it was also possible to achieve different lengths. The fibers percent incorporated were 0.05, 0.075, and 0.1. In some cases, 0.2 or even 0.3% were reached because optimum printability was still maintained at these higher values. The lengths of fibers used vary between 3 and 12 mm for short fibers, up to 20–30 mm for longer fibers. With all these properties, it was possible to analyze the rheological behavior in relation to the type, content, and length of the fibers.

Table 1 Mixtures of cement mortars and geopolymer mortars

Cement mortars									
Mixture	**1**	**2**	**3**	**4**	**5**	**6**	**7**	**8**	**9**
Cem III/B	24.50%	24.30%	24.60%	22.40%	22.00%	21.70%	-	-	-
Cem III/A	-	-	-	-	-	-	22.10%	22.00%	22.10%
Water	13.00%	14.00%	12.70%	12.70%	14.30%	15.20%	16.10%	16.60%	16.20%
Fly Ash	12.30%	12.10%	12.30%	13.10%	12.90%	12.80%	13.00%	12.90%	13.00%
Kaolin	1.00%	1.00%	1.00%	-	-	-	-	-	-
S.P	0.20%	0.20%	0.20%	0.20%	0.20%	0.30%	-	-	-
M.S	-	-	-	2.30%	2.20%	2.20%	-	-	-
N.S	-	-	-	0.60%	0.60%	0.60%	0.60%	0.60%	0.60%
Limestone [0–3]	49.00%	24.20%	24.60%	48.70%	23.90%	23.60%	-	-	-
Limestone [0–1]	-	-	-	-	-	-	48.20%	35.90%	36.10%
Seashells	-	24.20%	-	-	23.90%	-	-	12.00%	-
Glass	-	-	24.60%	-	-	-	-	-	-
CDW	-	-	-	-	-	23.60%	-	-	12.00%
Geopolymer mortars									
Mixture	**10**	**11**	**12**	**13**	**14**	**15**	**16**		
Fly Ash	27.10%	25.60%	27.20%	25.90%	25.50%	26.30%	27.60%		
NaOH [14 M]	11.60%	12.20%	11.80%	13.50%	14.60%	13.20%	-		
NaOH [10 M]	-	-	-	-	-	-	10.70%		
Water	1.60%	2.40%	1.80%	2.00%	2.60%	2.20%	-		
N.S	1.40%	1.30%	1.40%	1.30%	1.30%	1.30%	1.40%		
M.S	2.70%	2.60%	2.70%	2.60%	2.50%	2.60%	-		
S.P	1.40%	4.50%	0.70%	3.00%	2.50%	1.80%	-		
Limestone [0–3]	54.20%	25.70%	38.10%	-	-	-	55.20%		
Limestone [0–1]	-	-	-	51.70%	25.50%	36.80%	-		
Seashells	-	25.70%	-	-	25.50%	-	-		
Glass	-	-	16.30%	-	-	15.80%	-		

Table 2 Fiber characterization

	Length [mm]	Diameter [μm]	Density [g/cm3]	Tensile strength [MPa]	Modulus [GPa]	Elongation [%]
Aramid	6	21	1.39	3200	73	4.3
	12	21	1.39	3200	73	4.3
	20	420	1.35	2600	68	4.3
	30	420	1.35	2600	68	4.3
Carbon	6	7	1.8	4280	232	1.8
	25	7	1.78	4300	234	1.8
Cellulose	6	18–48	0.91	460	3.85	15
	20	18–48	0.91	460	3.85	15
Glass	13.1	13.5	2.68	1620	74	
Zylon	6		1.56	5800	270	2.5
Textile	20	150–170	1.24			
Polypropylene	6	31	0.91		1.5	

2.3 3D printer

For 3D printing, a WASP delta-type printer has been used, which is based on EMS technology and which helps, by superimposing layers, to manufacture different elements. This printer is made up of three articulated arms, arranged in a triangular configuration, which provides the printer with movement in the x, y, and z axes. These arms limit the maximum printing size to 1 m in height by 1 m in diameter. It also has a hopper into which the mortar is gradually poured. Inside this, there is the endless screw, which is connected to an electric motor, which permits the material to flow towards the nozzle. It has a circular section of 20 mm in diameter and is made of TPU to give it greater flexibility and grant a more fluid extrusion.

2.4 Rotational rheometer

To calculate the rheological parameters of fresh mortar mixes, a torque rheometer has been developed in the Universidad de Cantabria (UC). This will consist of three fundamental parts that are described below.

The setup consists of three main components. First, an agitator with adjustable rotation speeds ranging from 10 to 2000 rpm is connected to a computer, which records the torque corresponding to preset rotational speeds defined in the software. The agitator is mounted on a tripod using a clamp. Second, a 4-blade vane (cross-shaped), measuring 50 mm in height and 25 mm in radius, is attached to the agitator. Finally, a cylindrical steel container—sized appropriately based on the maximum aggregate size—is used to hold the mortar. The total cost of all components was under €2000.

Different authors have analyzed the relationship between the maximum aggregate size and the gap. Banfill et al. [19] established a maximum value for the ratio of 10 [19], while Laskar et al. [6] limited it to values between 3 and 10 [6], and Soualhi et al. [20, 21] defined through their tests that its optimal value is found from 5.

In addition, it is also established that the ratio between the inner diameter and the outside of the container must be lower than 1.2 [19]. With these relationships, two containers were made to help adapt to the different maximum aggregate sizes of the different mixtures to be analyzed. The first of them would be for dosages with a maximum aggregate size of 3 mm and would have an inner diameter of 80 mm and an outer diameter of 88 mm (gap/max. size = 5; D.ext/Dint = 1.19). The second one will be used for dosages with a maximum aggregate size of 1 mm and will have an inner diameter of 65 mm and an outer diameter of 72 mm. The height of the container in both cases was 150 mm. The cylinders were filled with mortar only 100 mm, and the blades were positioned on the first top half, so the upper boundary of the blades was air (see Fig. 1 (top)) and the bottom and side boundaries were mortar.

3 Methodology

3.1 Introduction

In order to check the validity of this non-commercial rheometer in the laboratory, preliminary 3D printing tests, numerical simulations, and a comparison with a commercial rheometer have been undertaken with mixtures without fibers.

Further rheological tests using the UC rheometer were conducted on different sustainable mortars containing fibers to analyze their influence in both shear stress and viscosity in order to define ranges that make the mixtures printable and buildable.

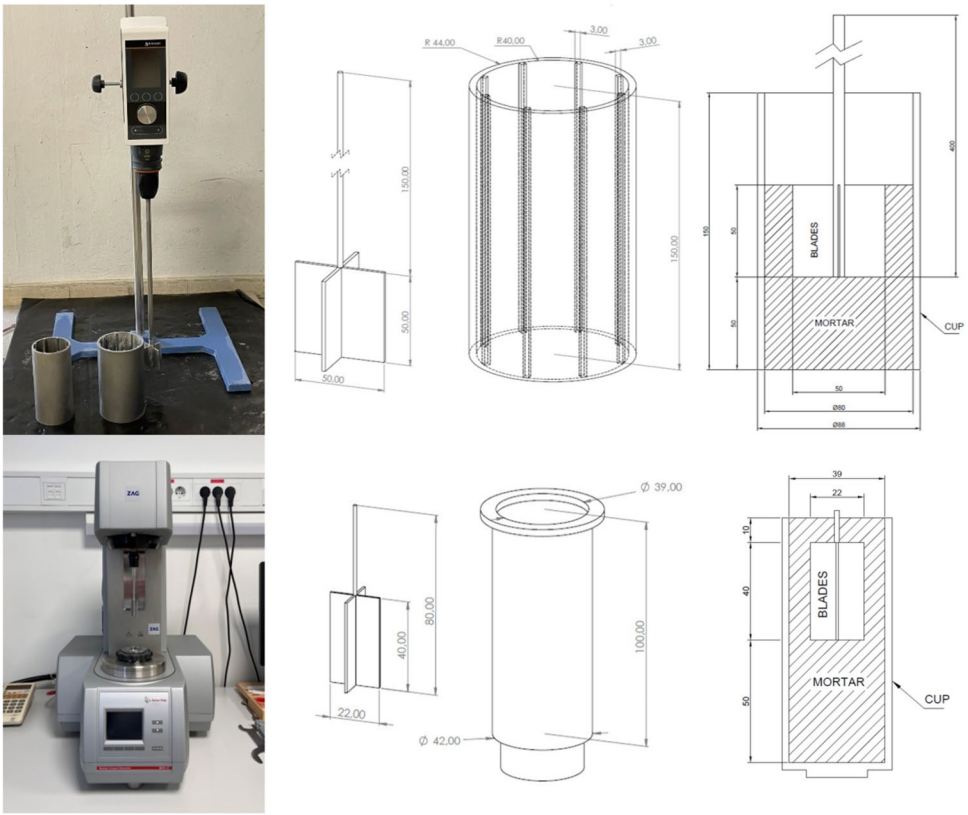

Fig. 1 Torque rheometers: UC own design (top), ZAG-Anton Paar MCR302 (bottom)

3.2 Preliminary printing trials

3D printing using extrusion relies on particular rheological characteristics of the mixtures while they are still in their fresh state. These properties should enable the material to guarantee workability and flowability, facilitating extrusion through the screw and nozzle of the 3D printer. However, after the layers have been extruded, they need to possess enough inner strength to keep their shape and bear the weight of upper layers. Therefore, initial printing trials were conducted to visually assess the suitability of various mortars for the purpose of printing (Fig. 2).

3.3 Rotational rheometer tests

3.3.1 Test procedure on mortars with and without fibers

The rheometer test consists of pouring a sample of fresh mortar in the cylindrical container, placing the blade in the center, and making it rotate at previously established decreasing speeds, while the torque data corresponds to each speed recorded. The data obtained are in the form of a linear equation and will help to obtain the yield stress and viscosity values, which are explained in the next section.

Before the test starts, some preliminary steps were carried out. First, the speed profile was defined for one of the reference printed samples, as established by [20, 21]. For this, the

Fig. 2 Preliminary printing trials

profiles 300, 257, and 200 were tested, being the profile 257 the one that is more stable, as it can be seen in Fig. 3 (left). In addition, it was observed that with 2-min duration, the samples had already stabilized.

Once the highest speed has been defined, the rest of the descending speeds that will form the profile are entered into the software, which is shown in Fig. 3 (right). With the profile already prepared, the tests are started with the reference sample, checking both that there is repeatability in them and that the values of the simulations show similar values to the test.

For each mixture, two samples (each sample is a new batch of the same mixture design) were tested/fabricated.

3.3.2 Calculation of yield stress and viscosity

When performing the tests with the rheometer, torque (M) and rotational speed (Ω) values are recorded by the equipment, which are linearly correlated. It is considered that the rheological behavior of mortar in a fresh state is that of a non-Newtonian fluid, which conforms in most cases to the Bingham model, governed by the following equation:$\tau = \tau_o + \eta\dot{\gamma}$, where τ_o is the yield stress and η refers to the viscosity of the mixture. In order to obtain these parameters, it is necessary to turn the values of torque-rotational speed measured with the equipment into values of shear stress-shear rate. For this, it is considered that the blade has a radius R_b and height h. Also, R_c will be the radius of the cup and Ω refers to the rotational speed of the vane. This allows to use the formulae proposed by Estellé et al. [22–24].

The shear rate, $\dot{\gamma}$, is calculated using Eqs. (1) and (2):

$$\dot{\gamma} = 2M\frac{d\Omega}{dM}, if\, \tau_c \le \tau_o \le \tau_b \tag{1}$$

$$\dot{\gamma} = 2\frac{M\frac{d\Omega}{dM}}{\left(1-\frac{R_b^2}{R_c^2}\right)} - \frac{\Omega - M\frac{d\Omega}{dM}}{\ln\left(\frac{R_b}{R_c}\right)}, if\, \tau_c > \tau_o \tag{2}$$

where τ_b and τ_c are the shear stresses on the inner and outer cylinders.

Obtaining as value of shear rate the maximum of the two previous equations.

$$\dot{\gamma} = \max(equation(1); equation(2)) \tag{3}$$

Moreover, the derivative dΩ/dM is approximated by Eq. (4):

$$\frac{d\Omega}{dM} = \frac{\Omega_j - \Omega_{j-1}}{M_j - M_{j-1}} \tag{4}$$

where j is the value corresponding to the rotation speed level and j-1 is the previous rotation speed level (decreasing rotation rate).

The wall shear stress,τ, which corresponds to the previously calculated shear rate, is obtained using the following equation:

$$\tau_b = \frac{M}{2\pi h R_b^2} \tag{5}$$

Once we obtained the shear stress–shear rate values with the formulae we have described, we can represent the curve, which will help to obtain the yield stress and viscosity values.

3.4 Numerical simulations methodology

Numerical simulations of the rheometer tests were carried out to study the Bingham model. The computational fluid

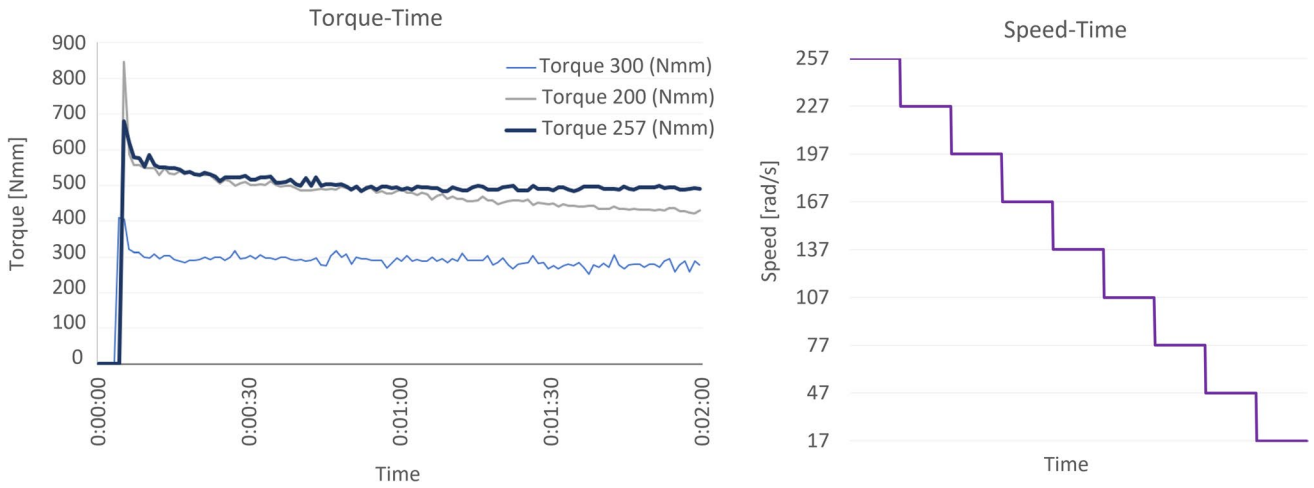

Fig. 3 Stabilization of profiles (left), 257 rotational speed profile (right)

dynamic (CFD) code FLUENT included in the software ANSYS Academic Research 20 R2 was used to simulate the rheometer blades moving and to calculate the torque acting on the fluid under testing conditions. The geometry of both the rheometer and the computational domain was defined with the ANSYS design modeler. Two diameter values of outer cylinder (80 mm and 65 mm) were used during experimental tests and, as a result, these were considered in the numerical simulation (Fig. 1 (top)). The lamellae located on the surface of the outer cylinder were not considered in the numerical calculations due to their low influence on shear flow in the region of fluid driven by the blades.

An air volume over the free surface of mortar tested was defined as part of the computational domain to regard the shear stress between both fluids. In addition, the top surface of blades is located at the same level of the surface between air and mortar; therefore, the air will influence the forces acting on the blades while they are rotating. The mesh of finite volumes was built both for the mortar region inside the rheometer and for the air region over the mortar with polyhedral cells (Fig. 4a). The advantages that polyhedral meshes have shown over some of the tetrahedral or hybrid meshes are the lower overall cell count, almost 3–5 times lower for unstructured meshes [25]. The number of cells is 233,195 and 266,511 for 65 mm and 80 mm of outer diameter, respectively. The fluid region closer to the blades surfaces is more densely meshed to capture properly the higher gradients in the flow variables due to friction between the fluid and solid surfaces. An inflated mesh was set in the boundary layer region to model the behavior of the fluid more accurately in this region. The rotational motion of the fluid and blades during the tests is simulated with a mesh that rotates at 17 rpm (Fig. 4c).

In the next step, the boundary conditions, the physical models, and the material properties were defined for the dynamic fluid analysis. Specifically, a wall condition was set for the boundary surfaces of the computational domain and the blades of the rheometer. The domain regions are shown in Fig. 4c; the height of the air region is 100 mm, and the height of the mortar region is also 100 mm. The mortar viscosity is described according to a Bingham model (a particular case of the Herschel-Bulkley model in ANSYS where $n = 0$ in the power law), whereas the air viscosity is fixed at 1.79×10^{-5} Pa·s.

A laminar flow was considered for the motion of fluids, and the interaction between the two phases (air and mortar) and their effect on the blades torque is estimated with the volume of fluid (VOF) model.

An unsteady analysis, 120 s long with a time step of 0.04 s, was carried out to estimate the torque generated by the blades. The equation of conservation of mass and momentum along with the physical models described above was solved by applying the finite volume method [26, 27]. Regarding the solution method, the PISO scheme was applied to solve the pressure–velocity coupling, and some second-order Upwind and PRESTO schemes were used for the spatial discretization.

3.5 Comparison with a commercial rheometer

As a final verification of the reliability of the new affordable rheometer developed by UC, a comparison with another commercial rheometer has been conducted with the collaboration of ZAG (Slovenian National Building and Civil Engineering Institute). The aim was to compare a mortar paste without fibers to check whether the UC rheometer provided similar results to a commercial rheometer. ZAG employed a commercial rheometer, Anton Paar MCR302 (4-blade type), with a cup diameter of 39 mm, blade height of 40 mm, and blade diameter of 22 mm.

A test protocol was established so that both UC and ZAG tested exactly the same material with the same procedure, in

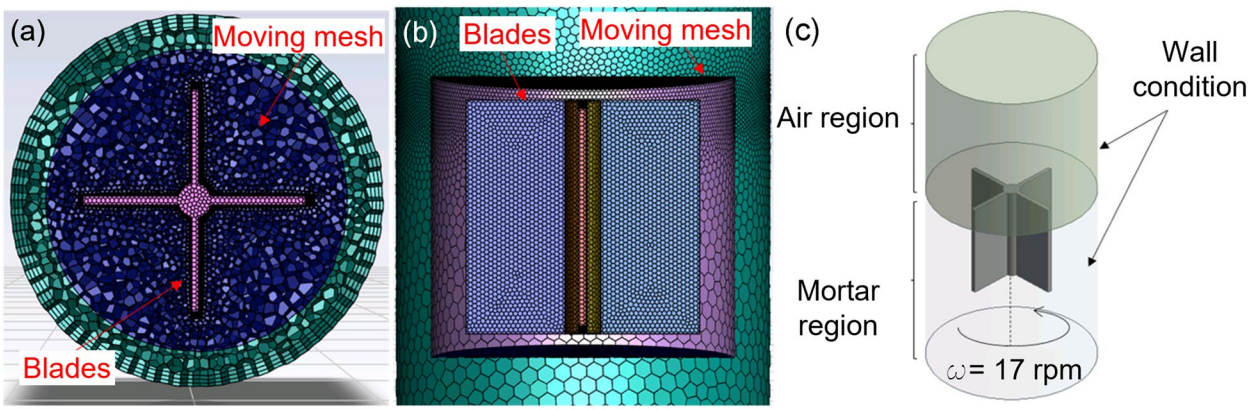

Fig. 4 Cross section views of mesh defined for the fluid domain regions: **a** top view and **b** side view. Domain regions and boundary condition defined in the numerical setup (**c**)

Table 3 Yield stress and viscosity of the mixtures without fibers

Mixture	Yield stress. Average [Pa]	Viscosity. Average [Pa•s]	Viscosity. Variation (%)	Yield stress. Variation (%)
1	592.81	12.98	4.20%	6.35%
2	508.03	11.48	1.12%	3.15%
3	399.54	15.01	1.07%	3.86%
4	237.83	11.25	0.65%	3.72%
5	305.78	11.30	0.44%	2.69%
6	322.33	14.41	0.05%	2.39%
7	345.28	5.24	1.12%	4.27%
8	360.39	4.18	2.76%	5.21%
9	171.70	6.82	4.83%	3.51%
10	636.79	14.18	0.07%	6.54%
11	564.67	11.47	2.12%	9.96%
12	533.71	11.37	2.06%	9.42%
13	347.31	14.64	1.10%	9.21%
14	424.57	10.84	1.74%	8.75%
15	496.62	11.59	2.24%	1.60%
16	569.55	22.44	0.05%	12.87%

such a way that it could be undertaken with both rheometers. The standard material used was a cement mortar, with the same composition of Mixture 1 in Table 1, with the exception of the superplasticizer that was changed: for the rheometer comparison, Belith S10 (admixture in powder) was used. UC delivered all the materials to ZAG to guarantee homogeneity of the mortars. The test procedure consisted of carrying out a rheological test for rotational rheometers using two methods for applying the rotational speed: step and ramp. The step method is based on the method proposed by [14] modifying the duration of each step and the pre-shear phase to adapt to the UC equipment. Detailed information about the test protocol and origin of materials is specified in the supplementary material for future potential replication. The values compared for the two rheometers are viscosity and yield stress, assuming a Bingham model. Five samples of each test were carried out, preparing always a new batch of fresh mortar. In the UC rheometer, values of shear stress and shear strain were calculated using expressions described in Sect. 3.3.2, while for the Anton Paar MCR302, shear stress and shear strain were calculated automatically by the equipment using its own conversion factors, CSS and CSR. CSS represents the conversion factor that transforms torque into shear stress, and CSR transforms rotational speed into shear strain. CSS and CSR were 93,850 Pa/(N*m) and 60 (s/s), respectively.

4 Results

4.1 Rheometer test results of mortars without fibers

Experimental results of all mixtures without fibers are summarized in Table 3, indicating average values and variations. Yield stress values varied from 171.70 to 636.79 Pa, while viscosity is comprised between 4.18 and 22.44 Pa•s. Figure 5 represents shear stress-shear rate curves of mixtures 1, 2, and 8, with two samples of each mixture. As it can be seen, shear stress vs shear rate varies linearly, with values of R^2 in the regression analysis that range from 0.9298 to 0.9953, showing that the Bingham model describes properly their behavior. Also, differences between two samples of the same mixture are relatively low. This trend is also maintained in the rest of the mixtures. Deviations of the rheological parameters present variations of the yield stress below 10% in all cases, while in the case of viscosity, they

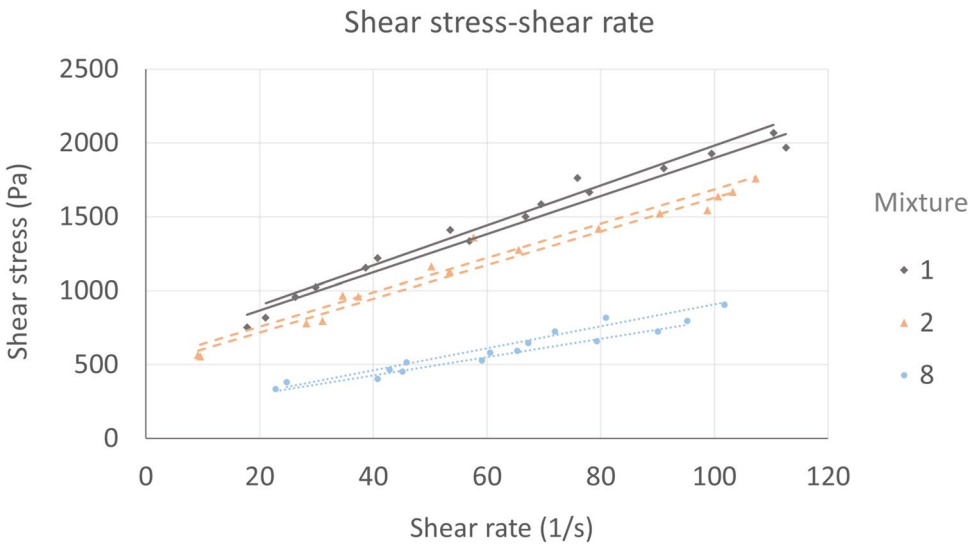

Fig. 5 Shear stress-shear rate of different mixtures

were even below 5% (Table 3). Therefore, this confirms a good repeatability of the test method and materials used.

Figure 6 shows that the tested mixtures have shear stress values ranging between 300 and 2000 Pa, while the shear rate values go from 10 to 120 s^{-1}. Yield stress is one of the rheological parameters that is most relevant in fresh mortar and especially when it is going to be used in 3D printing, since it indicates the force that the screw must exert to start the flow [28]. Banfill had already observed that the use of SP significantly reduced the value of yield stress [29]. In our case, it has been observed that if in addition to using SP, it is combined with two other workability modifiers, such as MS and NS, in cement mixtures, the yield stress value is even more reduced. Analyzing statistically the influence of adding workability modifiers admixtures in the yield stress, between mixtures 1, 2, and 3, which only incorporated SP, and 4, 5, and 6, in which MS and NS were also added, a *p*-value of 0.038 was obtained, lower than 0.05, which confirms that the incorporation of these admixtures significantly modifies the yield stress.

It can also be stated that the mixtures with the fine fraction aggregate [0–1] have lower yield stress values. The *p*-values both for the cement and geopolymer mixtures have been 0.03 and 0.043, respectively, both being lower than 0.05, confirming that the size of the aggregate significantly affects the decrease in the yield stress values.

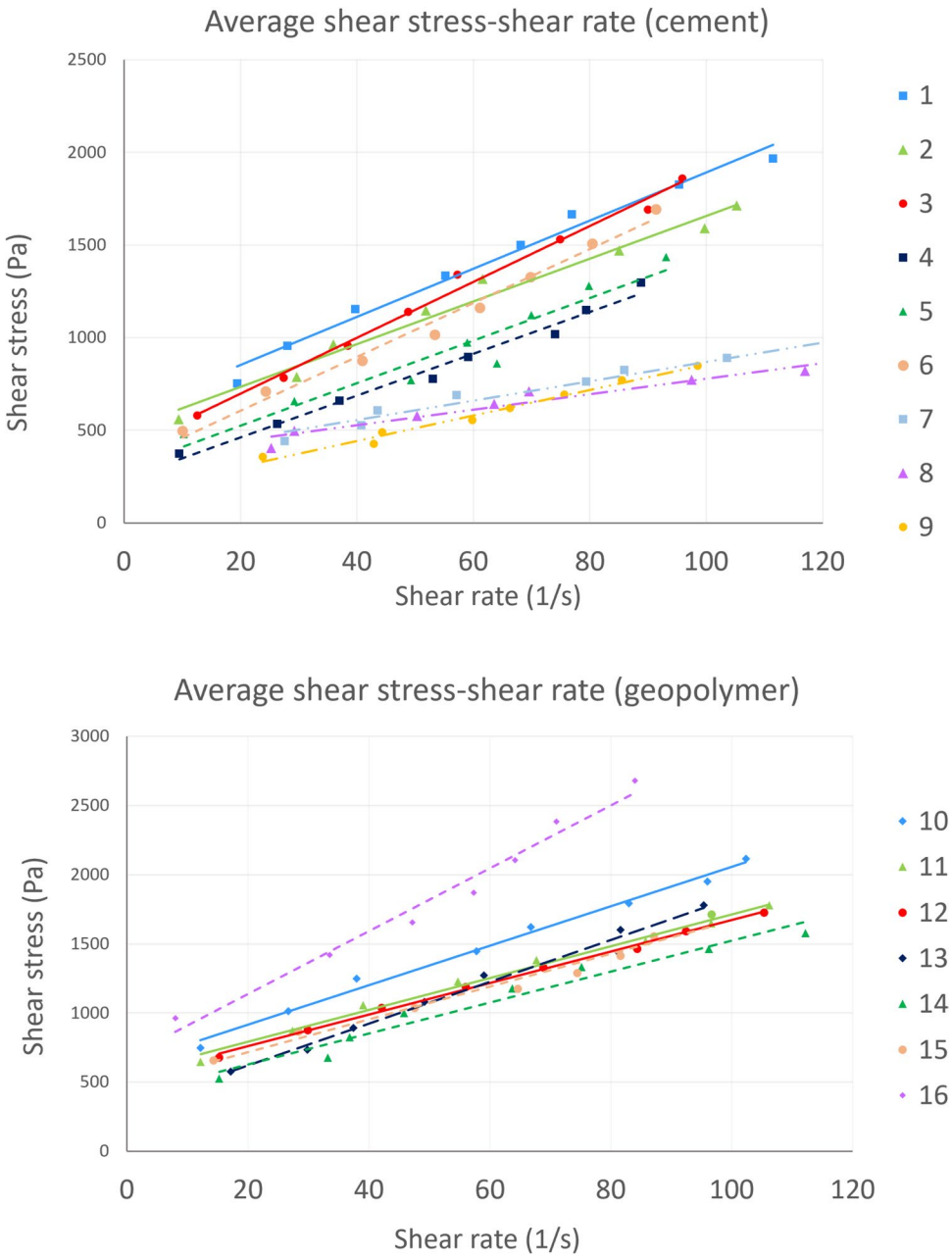

Fig. 6 Average shear stress-shear rate: cement (top), geopolymer (bottom)

Regarding the viscosity, it has been observed that the value range goes from 4.18 to 22.44 Pa•s. Mixtures with a low viscosity value also show some sort of dryness. Mixture 16 was the one that showed the largest stickiness in the laboratory, which also corresponds to the highest viscosity. In general terms, geopolymer mortars (mixes 10 to 16) tend to be stickier than cement mortars (mixtures 1 to 9), and this is also somehow correlated with their viscosity: viscosity in geopolymers is higher than in cement mortars.

In order to analyze how the mixtures' consistency changes over time, Fig. 7 shows the evolution of yield stress for Mixture 1 from the moment it is manufactured until 30 min later. The yield stress value for this time reached a value of 873 Pa, an increase of almost 50% with respect to the initial yield stress value. This time was selected because, in laboratory tests, after half an hour, the mixtures start to harden and the printer does not have enough strength to extrude the mixture, starting to produce choppy filaments or even getting the mixture set in the screw.

The increase in yield stress is considered to be linear until approximately 60 min [29], time after which it increases exponentially. Roussel et al. defined it by the following equation [29–31]:

$$\tau_o(t) = \tau_{o,o} + A_{thix}t$$

where A_{thix} is defined as the flocculation rate of the material and $\tau_{o,o}$ is the yield stress of the material with no time at rest.

The results obtained with our Mixture 1 show that it fits perfectly with the linear model proposed by Roussel, obtaining the following equation: $y = 577.02 + 9.5781x$, with a coefficient of determination R^2 of 0.982.

The values obtained in this work are also quite aligned with some previous works. For instance, Chen incorporated retarder admixtures into his mixtures, verifying that the yield stress values decrease as their quantity increases, obtaining yield stress values between 450 and 750 Pa [32]. Kolawole [33] and Banfill [34] analyzed how the mixtures behave with the incorporation of superplasticizer, concluding that this significantly reduces the yield stress values; however, these mixes were not meant to be used for 3D printing. The yield stress values obtained in this study align with those reported in the literature for 3DCP, which generally range between 100 and 800 Pa [12, 35] for dynamic yield stress.

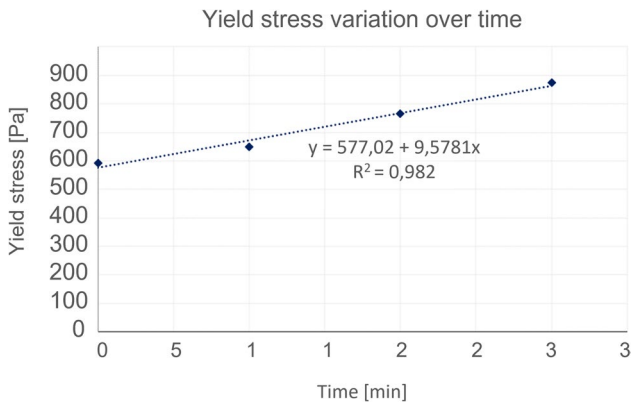

Fig. 7 Yield stress variation over setting time

4.2 Rheometer test results of mortars with fibers

The average results obtained after carrying out the tests three times per mixture are shown in Table 4. This made it possible to verify that the repeatability in these mixtures with fibers was maintained, as it was the case with the previously analyzed mixtures, with variations in yield stress of less than 10% and in viscosity of less than 5%. The yield stress values of the different samples range from 113.99 to 698 Pa and those of viscosity from 14.95 to 24.96 Pa•s.

Another aspect that was analyzed and which has been observed to have an important impact on the rheological results is the percentage of fibers that is incorporated in each of the mixtures. As shown in Table 4 (and statistically verified in Table 5), the yield stress values increase as the fiber content increases in all the types analyzed; consequently, the force to initiate flow that the 3D printer endless screw has to perform grows.

This also has a good correspondence with what is observed in the laboratory, since as a higher percentage of fibers was incorporated, the mixtures were printed in worse conditions, in some cases producing discontinuous filaments or even blocking the nozzle. Also, the mixtures with a greater quantity of fibers become drier, due to the fact that fibers absorb water affecting the workability of the mixture.

The highest percentage of fibers that was analyzed was that which allows printing correctly. Values above 700 Pa did not allow printing correctly. This threshold (700 Pa) was also observed in the tests analyzing the yield stress after different setting times (Fig. 7): after 20 min, the mixture was experiencing difficulties to be printed, which had a yield stress value of 765 Pa. Thus, it could be established that with values higher than 700 Pa printing problems begin to appear because the 3D printer screw does not have enough force to extrude the mixture.

Regarding the viscosity value, for each type of fiber and length, this has a tendency contrary to that of yield stress, since as the fiber content increases, the mixtures reduce the viscosity value. Despite this, it can be established that with viscosity values between 15 and 25 Pa•s, the mixtures with fibers are within the range of values that allow correct printing.

Finally, the influence of the length of the fibers and percentage added affecting the rheological behavior of the mortar were statistically analyzed, considering the input values

Table 4 Yield stress and viscosity of the mixtures with fibers

Material	Fibers length [mm]	Fibers percent [%]	Yield stress [Pa]	Viscosity [Pa•s]
Aramid	30	0.05	339.71	22.64
		0.075	445.67	21.83
		0.1	535.59	14.95
	20	0.05	250.33	24.11
		0.1	325.87	22.54
		0.2	473.98	22.11
	6	0.05	201.42	20.56
		0.075	247.65	18.97
		0.1	282.57	17.91
	12	0.05	113.99	17.64
		0.0625	327.89	16.12
		0.075	591.7	15.88
Glass	12	0.05	266.84	19.74
		0.1	491.98	18.82
		0.2	698.15	17.29
	13.1	0.1	185.01	23.97
		0.2	423.45	20.15
		0.3	571.77	17.96
Carbon	25	0.05	204.2	22.73
		0.075	358.03	21.15
		0.1	491.63	19.23
	6	0.05	199.05	22.67
		0.1	287.39	19.03
		0.2	451.01	18.72
Polypropylene	6	0.05	374.92	18.34
		0.075	425.76	18.21
		0.1	495.95	17.85
Cellulose	20	0.05	291.03	24.51
		0.075	421.99	21.14
		0.1	620.89	17.57
Zylon	6	0.05	247.46	24.96
		0.075	351.37	24.37
		0.1	472.49	23.28

Table 5 Correlations of rheological parameters with fiber type, length, and dosage

a) Coefficients and p-values of an ANOVA test

	Yield stress		Viscosity	
Terms	***p***-value	Significance ($p < 0.05$)	***p***-value	Significance ($p < 0.05$)
Material	0.195	No	0.060	No
Length (mm)	0.049	Yes	0.218	No
Percentage (%)	0.000	Yes	0.158	No

b) Regression models and determination coefficients

Dependent variable	Formulae	Determination coefficients
Yield stress (Pa) =	243.3 + 1392*Percentage (%)	33.47%

of Table 4. As shown in Table 5 (a), in terms of viscosity, no significant correlations were found with the material, fiber length, or percentage of fibers added to the mortar analyzing all materials and lengths as one single population. Regarding yield stress, a strong correlation was found with percentage, and a weaker correlation with fiber length. Nevertheless, when generating a regression model of yield stress vs percentage and length, the last one did not have a significant influence; thus, the model generated (see Table 5 (b)) only depends on fiber percentage. This means that the main parameter that drives the rheological behavior of mortars that contain fibers of different materials and lengths is the percentage of fibers added.

4.3 Numerical simulation results of mortars without fibers

The behavior pattern of mortar regarding pressure and velocity values is quite similar for all materials modeled in this work; thus, only the mixture 16 will be studied among all cases numerically simulated. Specifically, the material studied in this section is characterized by a viscosity of 22.4 Pa•s and a yield stress of 569.55 Pa. The pressure and speed values are obtained in three planes of cross section to the main axis of rotation of the blades during the test (Fig. 8a). These values are recorded once the torque produced by the blades stays in quasi-steady state (t = 120 s).

The higher values of mortar velocity are presented in the free surface between the air and mortar, where the mortar experiences a smaller resistance to its movement due to the lower viscosity of the air. Consequently, the mortar velocity decreases with the depth inside the container, reporting the lowest velocity values in the bottom plane of the blade. In the three levels studied, the mortar region where the velocity reaches the highest values is close to the blade tips, since the tangential velocity of blades increases with blade radius and, as a result, the transfer of moment will be higher.

The pressure values are quite constant in the free surface (top plane) and its average value is near zero, since the pressure is expressed as a relative pressure with respect to the atmospheric pressure and, consequently, the air presence affects significantly this pressure value. As the amount of mortar over the blades increases, a positive pressure is generated on one side of the blades and a negative pressure on the opposite side. This gradient of pressure mainly causes the force acting on the blades during the rotation, and hence the torque recorded both in the tests and the numerical simulations. As with velocity values, the pressure gradient is also higher near blade tips as a consequence of a higher moment transfer in this region, as it can be appreciated in Fig. 8f and g.

A comparison was made between the results obtained in the laboratory and the numerical simulation to assess the reliability of using the analytical formulas to convert rotational speed and torque into shear strain and shear stress. To do so, numerical simulations of the 16 mixtures without fibers were simulated introducing as input values the property of the fluid as a Bingham model, which were viscosity and yield stress obtained from the rheometer data and the analytical formulae described in Sect. 3.3.2. A rotational speed of 17 rpm was applied to the fluid in all the simulations. The output result from the numerical simulation was the torque calculated by the software, which was then compared with the torque value measured with the rheometer. Figure 9 shows the torque values obtained from the tests and from the CFD numerical simulation for the 16 mixtures. The errors obtained for the different materials in this comparison were in all cases lower than 15%. This confirms the good correlation between the test and the numerical simulation, which corroborates that the analytical formulae used to convert torque and rotational speed to shear stress and shear strain explained in Sect. 3.3.2 were adequate, validating the non-commercial rheometer developed at UC.

4.4 Comparison with a commercial rheometer

In Table 6, individual results of both rheometers with two methods (step method and ramp method) are shown. For each type of rheometer and method, coefficients of variations (CV) for viscosity are between 4.31 and 12.41% while for yield stress are higher, in the range of 9.79–36.37%.

It is important though to remark that Anton Paar MCR302 provides more similar values for viscosity and yield stress independently from the method used (step or ramp). Nevertheless, in terms of repeatability, UC rheometer is a bit more repetitive than Anton Paar MCR302 when the same method and material are used. However, since different operators perform the tests (UC operators with UC rheometer and ZAG operators with Anton Paar MCR302 rheometer), variability could also depend on that.

Since UC step method provides closer values of yield stress and viscosity to the ones of Anton Paar MCR302, this justifies somehow the methodology adopted in this paper in previous sections to select step method rather than ramp method. Nevertheless, UC rheometer still provides higher values of viscosity (around 10% higher for step method) and lower values of yield stress (around 46% lower for step method) compared to Anton Paar MCR302. Since the actual value of the mortar is unknown, it is difficult to infer which of the two rheometers is more accurate.

Haist et al. [14] developed an interlaboratory study on rheological properties that was conducted for a cement paste using 25 different commercial rheometers. An ultrasonic gel was used as a standard material by all laboratories to define conversion factors to correlate yield stress with torque and shear rate with rotational speed and to be able to compare all

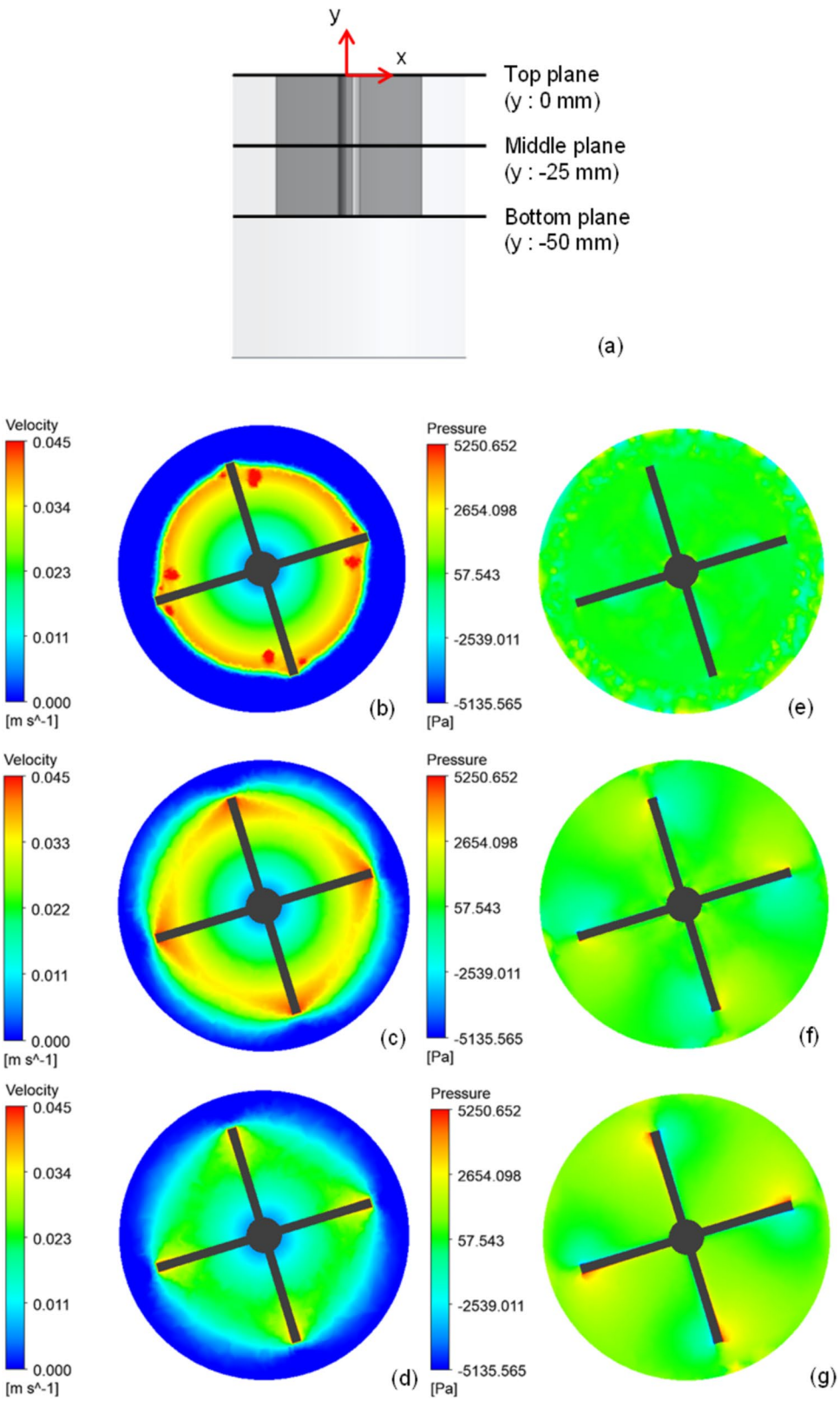

Fig. 8 Cross section plans where the pressure and velocity values are obtained (**a**). Contour map of velocity and pressure at the following depth values from the mortar surface: 0 mm (**b** and **e**); − 25 mm (**c** and **f**), and − 50 mm (**d** and **g**)

rheometers even though they had different shearing systems and geometries. A downward step flow curve was applied in all rheometers following an agreed protocol. The values of viscosity ranged between 0.33 and 0.90 Pa•s and from 2.10 to 66.51 Pa for yield stress. The averaged values of all laboratories (excluding five outliers) were 0.5 Pa•s ± 0.12

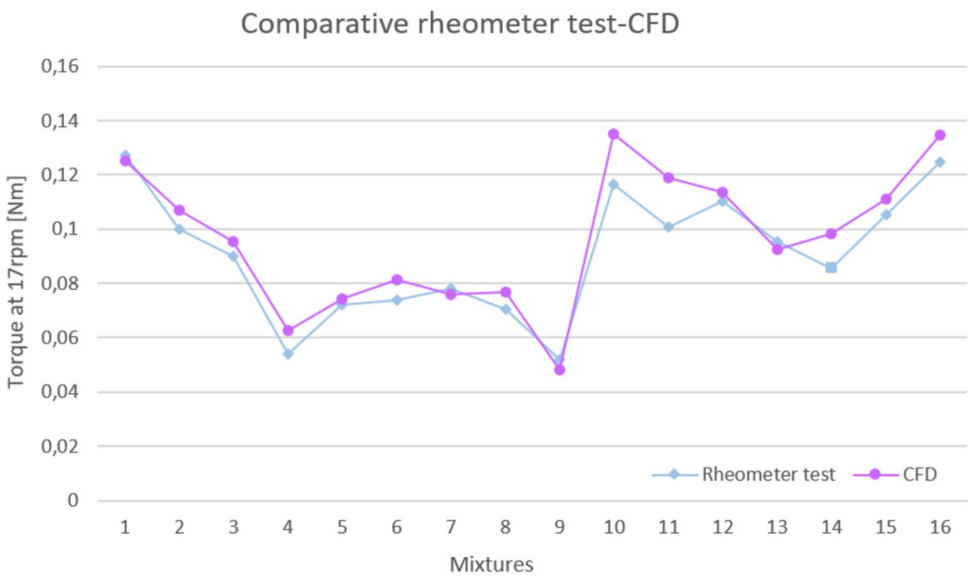

Fig. 9 Comparative rheometer test—CFD numerical simulation

Table 6 Comparison of viscosity and yield stress of different rheometers (step and ramp methods)

	Step method				Ramp method			
	UC Own design		Anton Paar MCR302		UC Own design		Anton Paar MCR302	
	Yield stress (Pa)	Viscosity (Pas)	Yield stress (Pa)	Viscosity (Pas)	Yield stress (Pa)	Viscosity (Pas)	Yield stress (Pa)	Viscosity (Pas)
1	442.11	9.45	516.82	8.64	566.08	10.73	500.75	9.79
2	247.68	9.39	712.06	9.22	494.62	11.71	311.71	9.15
3	538.25	7.94	324.62	9.70	575.85	10.64	712.50	7.40
4	277.68	10.40	614.40	7.65	652.71	10.85	900.26	8.61
5	533.40	9.91	817.94	7.20	570.66	11.48	761.38	7.44
AVGE	407.83	9.42	597.17	8.48	571.98	11.08	637.32	8.48
ST.DV	138.33	0.92	189.06	1.05	56.02	0.48	231.76	1.05
CV (%)	33.92	9.77	31.66	12.35	9.79	4.31	36.37	12.41

AVGE average, *ST.DV.* standard deviation, *C.V. (%)* coefficient of variation expressed in percentage

Pa•s for the viscosity and 40.0 Pa ± 10.97 Pa for the yield stress. The variability values (measured through standard deviation) imply that there is a 24% coefficient of variation for the viscosity and 27.4% for the yield stress. Among these rheometers, they also used an Anton Paar MCR302 rheometer (blade height, 40 mm; blade diameter, 22 mm; cup diameter, 28.9 mm) whose results were 0.55 Pa•s for the viscosity (10% higher than the average of all labs) and 40.57 Pa for the yield stress (1.4% higher than the average of all labs). The actual values of viscosity and yield stress of the cement paste are unknown since it is not a standard material.

In order to quantitatively compare the results of both UC and ZAG laboratories with different equipment and flow curves (ramp vs step), statistical analysis has been done in the same way as when conducting proficiency tests; results are shown in Table 7. To undertake the comparison, ISO 13528 [36] has been followed. In this case, four tests have been compared: UC-step method, ZAG-step method, UC-ramp method, and ZAG-ramp method, and for each of them, two values: yield stress and viscosity. To estimate the central value instead of the average, the

Table 7 Z-score of the tests according to ISO 13528-Annex C

	Yield stress (Pa)	**Z-score** (x_i-median)/nIQRX	**Viscosity (Pas)**	**Z-score** (x_i-median)/nIQRX
UC-step	407.83	−1.87	9.42	0.36
ZAG-step	597.17	0.13	8.48	−0.36
UC-ramp	571.98	−0.13	11.08	1.62
ZAG-ramp	637.32	0.56	8.48	−0.36
Median	584.58		8.95	
nIQRX	94.40		1.31	

median has been taken, as recommended in ISO 13528-Annex C, when few data are compared. In the same way, the estimator for the dispersion recommended in the standard when analyzing a short set of values is the normalized interquartile range (nIQRX), which is expressed as 0.7413 (Q_3-Q_1), where Q_3 and Q_1 represent the 75th percentile and 25th percentile, respectively. Then, the Z score is calculated according to ISO 13528: each laboratory value minus the median and divided by the nIQRX. If the Z-score is < 2, it means that the parameter is considered valid. As it can be seen in Table 7, all values are < 2.0; nevertheless, values from UC (UC own design rheometer) show higher Z-score values than those from ZAG (Anton Paar MCR302 rheometer).

Overall, despite the high variability typically associated with rheological measurements—due to material inconsistencies, differences in rheometers, testing methods, or operator handling—the UC low-cost rheometer produces reasonably accurate results, as confirmed by z-score validation. Additionally, numerical simulations align well with the experimental data, which supports the validity of the analytical formulas used to convert measured parameters (rotational speed and torque) into rheological values (shear stress and strain rate). This further confirms the reliability of the viscosity and shear stress results based on the Bingham model.

5 Conclusions

This study analyzed the rheological behavior of various mixture dosages used in extrusion-based printing, with a particular focus on how fiber incorporation affects performance. The mixtures were experimentally evaluated using a custom-developed torque rheometer, whose functionality was validated through numerical simulations. Based on the findings, the following conclusions were drawn:

- The UC rheometer provides results that are consistent and acceptable when compared to a commercial rheometer, such as the Anton Paar MCR302.
- CFD simulations have proven to be a powerful tool for analyzing the behavior of Bingham fluids and predicting the torque generated by the rheometer blades. The difference between experimental and simulated torque values remains within 15%.
- The use of workability-enhancing admixtures—such as superplasticizer, nanosilica, and microsilica—significantly reduces the yield stress of the mortar. Among these, the superplasticizer has the greatest impact.
- The inclusion of fine aggregates (0–1 mm fraction) also contributes to a reduction in yield stress, both in cement and geopolymer mixtures.
- Geopolymer mixtures exhibit higher viscosity than cement-based mortars, which correlates with a noticeable increase in stickiness.
- The addition of fibers significantly affects yield stress. As fiber content increases—regardless of the fiber type—the yield stress also increases. Furthermore, yield stress tends to rise linearly with setting time. When the yield stress exceeds approximately 700 Pa, printing issues such as filament discontinuity or nozzle blockage occur in WASP Delta-type 3D printers.
- Among all parameters, fiber content has the greatest influence on yield stress. However, no clear correlation is observed between viscosity and fiber type, length, or dosage.
- For extrusion-based 3D printers like the WASP Delta, optimal viscosity values range from 5 to 25 Pa·s. Higher values correspond to stickier mixes, while lower values result in drier mixes. Similarly, ideal yield stress values fall between 100 and 700 Pa; exceeding this range can compromise print quality or lead to printer malfunction.

Supplementary Information The online version contains supplementary material available at https://doi.org/10.1007/s00170-025-16244-w.

Acknowledgements The authors would like to thank the following companies for their contributions: Cementos Portland Valderribas S.A. for providing the cement, Solvay for providing the fly ash and NaOH, Basf Chemicals Ltd. and BECSA for providing additives, Teijin Ltd. for providing various types of fibers (aramid, carbon and zylon), Fibratec Técnicas de la Fibra S.L for providing the glass fibers, and Textil Santanderina S.A. for providing the textile fibers.

Funding Open Access funding provided thanks to the CRUE-CSIC agreement with Springer Nature. The work has received funding by the Spanish Ministry of Science and Innovation through four grants: • *"Promotion of activity in R + D of GITECO and GCS groups of the University of Cantabria" (Ref: SSPJO1900I001723XV0).* • *"Fostering the circular economy and low CO2 technologies through the additive manufacturing −3DCircle" (Ref: PID2020-112851RA-I00).* • *"Enhancing biodiversity in the Atlantic area through sustainable artificial reefs -EBASAR-" (Ref: TED2021-129532B-I00).* • *"Holistic approach to foster circular and resilient transport infrastructures and support the deployment of green and innovation public procurement and innovative engineering practices -CIRCUIT-" (Ref: HORIZON-CL5-2022-D6-02 No.101104283).*

Declarations

Ethical approval This article does not contain any studies with human participants or animals performed by any of the authors.

Conflict of interest The authors declare no competing interests.

References

1. Tay YWD, Panda B, Paul SC, Mohamed NAN, Tan MJ, Leong KF (2017) 3D printing trends in building and construction industry: a review. Virtual Phys Prototyp 12(3):261–276. https://doi.org/10.1080/17452759.2017.1326724
2. Pegna J (1997) Exploratory investigation of solid freeform construction. Autom Constr 5(5):427–437. https://doi.org/10.1016/S0926-5805(96)00166-5
3. Wallevik JE (2006) Relationship between the Bingham parameters and slump. Cem Concr Res 36(7):1214–1221. https://doi.org/10.1016/j.cemconres.2006.03.001
4. G. H. Tattersall and P. F. G. Banfill (1983) The rheology of fresh concrete. Pitman Advanced Publishing Program
5. de Matos PR, Pilar R, Casagrande CA, Gleize PJP, Pelisser F (2020) Comparison between methods for determining the yield stress of cement pastes. J Braz Soc Mech Sci Eng. https://doi.org/10.1007/s40430-019-2111-2
6. Laskar AI, Bhattacharjee R (2011) Torque-speed relationship in a concrete rheometer with vane geometry. Constr Build Mater 25(8):3443–3449. https://doi.org/10.1016/j.conbuildmat.2011.03.035
7. E. P. Koehler and D. W. Fowler (2004) "Development of a portable rheometer for fresh portland cement concrete," Research Report ICAR –105–3F
8. Domone PLJ, Yongmo Xu, Banfill PFG (1999) Developments of the two-point workability test for high-performance concrete. Mag Concr Res 51(3):171–179. https://doi.org/10.1680/macr.1999.51.3.171
9. O. H. Wallevik and O. H. Gjorv (1990) "Development of a coaxial cylinder viscometer for fresh concrete," Properties of fresh concrete, Proceeding of RILEM Colloquium
10. F. Larrard, J. C. Szitkar, C. Hu, and M. Joly (1996) "Evolution of the workability of superplasticized concrete: assessment with the BTRHEOM rheometer," in RILEM Intern Conf Prod Meth Work Concr
11. F. de Larrard, J.-C. Szitkar, and C. Hu (1993) "Design of a rheometer for fluid concretes | Conception d'un rheometre pour betons fluides," Bulletin de liaison des laboratoires des ponts et chaussees no. 186: pp. 55–59
12. Jayathilakage R, Rajeev P, Sanjayan J (2022) Rheometry for concrete 3D printing: a review and an experimental comparison. Buildings. https://doi.org/10.3390/buildings12081190
13. L. E. Brower and C. F. Ferraris (2006) "Comparison of concrete rheometers," in ACI Special Publication pp. 117–135
14. Haist M et al (2020) Interlaboratory study on rheological properties of cement pastes and reference substances: comparability of measurements performed with different rheometers and measurement geometries. Mater Struct. https://doi.org/10.1617/s11527-020-01477-w
15. M. Eslami Pirharati, D. Ivanov, H.-W. Krauss, C. Schilde, and D. Lowke (2020) Numerical simulation of the flow behavior of Newtonian fluids in a wide gap rheometer by CFD vol. 23 https://doi.org/10.1007/978-3-030-22566-7_68.
16. J. E. Wallevik (2016) "Parallel plate based measuring system for the ConTec viscometer rheological measurement of concrete with D max 32 mm," Reykjavik
17. Boddepalli U, Panda B, Gandhi ISR (2023) Rheology and printability of Portland cement based materials: a review. J Sustain Cem Based Mater 12(7):789–807. https://doi.org/10.1080/21650373.2022.2119620
18. Alonso-Cañon S, Blanco-Fernandez E, Castro-Fresno D, Yoris-Nobile AI, Castanon-Jano L (2024) Comparison of reinforcement fibers in 3D printing mortars using multi-criteria analysis. Int J Adv Manuf Technol 134(3–4):1463–1485. https://doi.org/10.1007/s00170-024-14126-1
19. P. F. G. Banfill (2003) "The rheology of fresh cement and concrete – a review," in Proc 11th Intern Cem Chem Congr
20. H. Soualhi, E. H. Kadri, T.-T. Ngo, A. Bouvet, F. Cussigh, and S. Kenai (2014) "A vane rheometer for fresh mortar: development and validation," Appl Rheol vol. 24(no. 2) https://doi.org/10.3933/ApplRheol-24-22594.
21. Soualhi H, Kadri E-H, Ngo T-T, Bouvet A, Cussigh F, Tahar Z-E-A (2017) Design of portable rheometer with new vane geometry to estimate concrete rheological parameters. J Civ Eng Manag 23(3):347–355. https://doi.org/10.3846/13923730.2015.1128481
22. Lanos C, Estellé P (2009) Vers une réelle rhéométrie adaptée aux bétons frais. Rev Eur Genie Civil 13(4):457–471. https://doi.org/10.3166/ejece.13.257-471
23. Estellé P, Lanos C, Perrot A (2008) Processing the Couette viscometry data using a Bingham approximation in shear rate calculation. J Nonnewton Fluid Mech 154(1):31–38. https://doi.org/10.1016/j.jnnfm.2008.01.006
24. P. Estellé, C. Lanos, A. Perrot, and S. Amziane (2008) "Processing the vane shear flow data from Couette analogy,". Appl Rheol vol. 18(no. 3) https://doi.org/10.1515/arh-2008-0009.
25. ANSYS (2021) Ansys fluent workbench tutorial guide. ANSYS, Inc., Canonsburg, PA, USA
26. B. Andersson, R. Andersson, L. Håkansson, M. Mortensen, R. Sudiyo, and B. Van Wachem (2011) Computational fluid dynamics for engineers vol. 9781107018 https://doi.org/10.1017/CBO9781139093590.
27. J. Tu, G.-H. Yeoh, and C. Liu (2018) Computational fluid dynamics: a practical approach
28. Panda B, Unluer C, Tan MJ (2018) Investigation of the rheology and strength of geopolymer mixtures for extrusion-based 3D printing. Cem Concr Compos 94:307–314. https://doi.org/10.1016/j.cemconcomp.2018.10.002
29. Roussel N (2005) Steady and transient flow behaviour of fresh cement pastes. Cem Concr Res 35(9):1656–1664. https://doi.org/10.1016/j.cemconres.2004.08.001
30. Roussel N (2006) A thixotropy model for fresh fluid concretes: theory, validation and applications. Cem Concr Res 36(10):1797–1806. https://doi.org/10.1016/j.cemconres.2006.05.025
31. Roussel N (2018) Rheological requirements for printable concretes. Cem Concr Res 112:76–85. https://doi.org/10.1016/j.cemconres.2018.04.005
32. M. Chen et al (2020) "Rheological parameters and building time of 3D printing sulphoaluminate cement paste modified by retarder and diatomite," Constr Build Mater vol. 234 https://doi.org/10.1016/j.conbuildmat.2019.117391.
33. Kolawole JT, Combrinck R, Boshoff WP (2019) Measuring the thixotropy of conventional concrete: the influence of viscosity modifying agent, superplasticiser and water. Constr Build Mater 225:853–867. https://doi.org/10.1016/j.conbuildmat.2019.07.240
34. Banfill PFG (2011) Additivity effects in the rheology of fresh concrete containing water-reducing admixtures. Constr Build Mater 25(6):2955–2960. https://doi.org/10.1016/j.conbuildmat.2010.12.001

35. Rehman UA, Kim J-H (2021) 3D concrete printing: a systematic review of rheology, mix designs, mechanical, microstructural, and durability characteristics. Materials. https://doi.org/10.3390/ma14143800
36. International Organization for Standardization (2022) ISO 13528:2022.Statistical methods for use in proficiency testing by interlaboratory comparison